An Inquiry on Contrast Enhancement Methods for Satellite Images

Jose-Luis Lisani, Julien Michel, Jean-Michel Morel, Ana Belén Petro, and Catalina Sbert

***Abstract*—Enhancement algorithms are absolutely necessary for the visualization of both shadowed and bright image regions. Defining algorithms that permit to visualize them simultaneously without altering the image content is therefore extremely relevant for remote sensing applications. In this paper, we present the results of two successive benchmarks which tested the performance of the state-of-the-art contrast enhancement and tone-mapping algorithms applied to satellite images. Experts from the French Space Agency Centre National d'Etudes Spatiales (CNES), Service Régional de Traitement d'Image et de Télédétection (SERTIT), and two European universities assessed the quality and fidelity of the results of several state-of-the-art enhancement algorithms on the excerpts from seven images (five Pleiades and two simulated 30-cm images). The first benchmark permitted to tighten the procedure and the selection of the test images for the second one, and to make a first selection of concurrent algorithms. The second benchmark not only included the best algorithms selected by the first benchmark but also added even more competitors in the tone-mapping class. The results of both benchmarks were coherent. They point a particular retinex-based algorithm as the best compromise between the competitive requirements of a contrast enhancement in dark regions and a preservation of detail in bright parts.**

***Index Terms*—Geophysical image processing, image color analysis, image enhancement.**

I. Introduction

In [1], Campbell defined remote sensing as "the practice of deriving information about the Earth's land and water surfaces using images acquired from an overhead perspective, using electromagnetic radiation in one or more regions of the electromagnetic spectrum, reflected or emitted from the Earth's surface." Satellite images literally and figuratively give us a different way of looking at the world [2]. However, because of this unfamiliar perspective and of values obtained from radiation outside the visible portion of the electromagnetic spectrum, such images require a specific rendering to adapt to human vision.

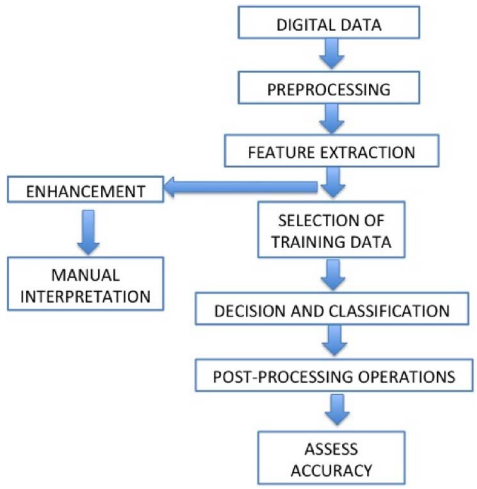

Fig. 1. Idealized sequence for digital analysis in remote sensing. Extracted from [1, Fig. 4.19, p. 117].

Furthermore, a satellite sensor must capture a wide range of scenes, from very low radiance (oceans, low solar elevation angles, high latitudes) to very high radiance (snow, sand, high solar elevation angles, and low latitudes) [3]. As a result, the quantization can be coarse, and any given image will generally occupy only a limited portion of the available dynamic range, therefore having low contrast [2]. Moreover, the energy reaching the satellite must pass through the entire depth of the Earth's atmosphere. Atmospheric effects may also reduce the dynamic range. For example, the particles suspended in the atmosphere or large molecules of atmospheric gases can redirect the electromagnetic waves (an effect called scattering), modifying the final images and affecting the vision in the shadows [1]. Thus, rendering these images to human observers systematically requires the use of a contrast enhancement method.

An enhanced visualization of the satellite images is not the sole goal of the image processing chain. In many cases, these images are fed into a postprocessing block to extract useful information.

Fig. 1 depicts the idealized sequence for digital analysis.

As we can observe, after the preprocessing is complete, the analyst may choose to apply techniques to improve the visual appearance of the image, using image enhancement to prepare the image for subsequent manual interpretation. Because image enhancement often drastically alters the original numerical data, it is normally used only for visual (manual) interpretation and not for further numerical analysis [1]. For

Manuscript received April 18, 2016; revised July 5, 2016; accepted July 20, 2016. Date of publication August 19, 2016; date of current version September 30, 2016. This work was supported in part by the Centre National d'Études Spatiales through the Mathématiques de l'Imagerie Stéréoscopique Spatiale (MISS) Project, by the European Research Council Advanced Grant through the Twelve Labours Project, by the Office of Naval Research under Grant N00014-97-1-0839, and by the Ministerio de Economía y Competitividad under Grant TIN2011-27539 and Grant TIN2014-53772.

J.-L. Lisani, A. B. Petro, and C. Sbert are with Universitat de les Illes Balears, 07122 Palma, Spain (e-mail: joseluis.lisani@uib.es; anabelen.petro@uib.es; catalina.sbert@uib.es).

J. Michel is with Centre National d'Etudes Spatiales, 31400 Toulouse, France (e-mail: julien.michel@cnes.fr).

J.-M. Morel is with Centre de Mathématiques et de leurs Applications, École Normale Supérieure de Cachan, 94235 Cachan, France (e-mail: moreljeanmichel@gmail.com).

Color versions of one or more of the figures in this paper are available online at http://ieeexplore.ieee.org.

Digital Object Identifier 10.1109/TGRS.2016.2594339

Fig. 2. Some typical problems of the satellite images can be observed in these two examples (CNES 2014, CNES 2012). (Left) Color cast and shadows. (Right) Haze and shadows.

example, shadows are a clue in the interpretation of objects. A shadow may reveal the characteristics of size or shape that would not be obvious from the overhead view alone [1]. Thus, image enhancement must attenuate but not eliminate shadows.

In this paper, we focus on the enhancement seen as a way to foster image detail visualization without altering its structure. In satellite imaging, the "quality of an image" is, conventionally, the ability of an image to meet the user's needs [4]. However, the needs are not the same and depend on the applications involved (photo interpretation, mapping, agricultural monitoring, radiation balance, meteorology, water color, etc.), and the concept of image quality can therefore fluctuate from a project to the other. For example, shadows are often thought of in a negative sense by photo interpreters because it can be difficult to see objects in deep shadows [2], but for mapping, as we have mentioned earlier, shadows provide information about the height profile of objects.

We observed that, in general, the satellite or remote sensing images usually present more than just one specific contrast problem. As can be observed in the examples displayed in Fig. 2, it is common to find images containing color cast and shadows or images presenting both shadows and fog.

The contrast problem is not specific to satellite imaging. Contrast enhancement is one of the most important issues in image processing. Among all image processing techniques, it is the one that has the strongest impact on image quality. Many contrast enhancement techniques have therefore been proposed to improve image contrast.

Despite the vast literature on contrast enhancement methods, few references on the application of these methods to cases of remote sensing or satellite images can be found. Some recent contributions are [5]–[8]. The first two studies deal with the case of uneven illumination in remote sensing images. Li *et al.* [5] proposed a perceptually inspired variational method that uses multiple priors (L^2 norm and total variation) at the contrast term and the Gray World assumption in the dispersion item of the functional. The proposed method is very similar to the ACE algorithm (see Section II-A), and the results are compared with a variational implementation of the retinex theory. The drawback of this method is that it is time-consuming, and the parameters weighting each item are manually determined. Liu *et al.* [6] presented an image-balancing technique that adjusts the mean and standard deviation of a neighborhood at each pixel and consists of three steps, namely, elimination of coarse light background, image balancing, and max–mean–min radiation correction. According to the authors, the main limitation of their method is that it is more time-consuming than previously existing techniques. Finally, Lee *et al.* [8] and Jang *et al.* [7] applied methods in which the image is decomposed into subbands or band-limited components, and then, they used a contrast enhancement function to better perceive details. The first work is based on the discrete wavelet transform, and the second one on multiscale retinex (see Section II-A).

The aim of this paper is to test the performance of the state-of-the-art contrast enhancement and tone-mapping algorithms applied to satellite images. Similar studies have been performed on pictorial nonsatellite images [9], [10] or in synthetic aperture radar images [11]. However, as mentioned earlier, the characteristics of satellite images are different from those of other types of images. Most importantly, the analysis and interpretation by the photo interpreters of these images are very peculiar. For example, the principal visually annoying artifacts that can be found in an image are noise, halo, low contrast, and false colors. These artifacts can be attenuated or amplified depending on the contrast enhancement method. In art photography or user-level photography, halos or noise are undesirable artifacts. However, photo interpreters are not usually bothered by such effects since they are able to recover the important information on the image without removing them. In fact, they prefer to work with images, as close as possible to the original, without postprocessing since this processing may introduce new unwanted artifacts. The only acceptable processing for a photo interpreter is such that it improves the visibility in dark regions while preserving the details in bright regions, which may be lost due to an excessive saturation. This processing permits to get the maximum information from the satellite image. Under these considerations, we shall analyze well-known contrast enhancement and tone-mapping methods to improve the contrast enhancement of satellite images.

Our benchmark was an extensive inquiry with two successive stages. We first established a list of representative state-of-the-art image enhancement methods. We performed an initial study with these classical algorithms to detect the "needs" of the users, by using a simple voting scheme among the interpreters of the satellite images. We also obtained comments from photo interpreters about the reasons of their ratings which oriented the second benchmark. From some initial conclusions and using psychometric scaling techniques [12], we devised this second benchmark, fixing the judgment task of the observers and extending the algorithms to various state-of-the-art tone-mapping methods using a fixed set of input subimages. In order to better discriminate the reasons why some methods were favored over others, we invited the experts to separately rate the overall contrast but also to pay a special attention to the loss of contrast in bright areas, resulting in an apparent saturation. Finally, observing that color visualization had been a concurrent quality criterion interfering with contrast criteria, we decided to separate the study of contrast enhancement from that of color enhancement by using only grayscale images in the second benchmark. Thus, the second benchmark is focused on the enhancement of brightness, which allows experts to assess the improvement in contrast independently of the color quality. Let us stress that a study on contrast perception in

TABLE I
HISTOGRAM-BASED METHODS

Name	Description	Advantages	Disadvantages
Simplest Color Balance (SCB, [14])	$T_{SCB}(u) = \frac{u-u_{min}}{u_{max}-u_{min}}$, $\#\{\mathbf{x} : u(\mathbf{x}) \leq u_{min}\} = s_1\%$ of N, $\#\{\mathbf{x} : u(\mathbf{x}) \geq u_{max}\} = s_2\%$ of N	Good results in satellite images, with small clipping percentages.	Saturation can create flat white regions or flat black regions that may look unnatural. Parameters: s_1 and s_2 (clipping percentages).
Histogram Equalization (HE)	$T_{HE}(u) = F(u)$, $F(l) = \frac{\#\{\mathbf{x}:\, u(\mathbf{x}) \leq l\}}{N}$	Increases the global contrast. No parameters	Excessively reveals noise and quantization.
Piecewise Equalization (PE, [15])	$T_{PE}(u) = F_{k'}(u), \quad l_{k'} \leq u \leq l_{k'+1}$ $F_k(l) = z_k + m_k(l - l_k)$, $k = 0, 1, \ldots, M$ $z_k = k/M$, $l_k = F^{-1}(z_k)$, $m_k = \max(s_{min}, \min(s_{max}, \frac{z_{k+1}-z_k}{l_{k+1}-l_k}))$,	Limits the SNR, local degradation, and color attenuation.	Slope too small, contrast reduction Slope too large, noise amplification. Parameters: M, s_{min}, s_{max}.
Ideal Gamma (IG)	$T_{IG}(u) = \left(\frac{u-u_{min}}{u_{max}-u_{min}}\right)^{\gamma}$, γ s.t. $\frac{1}{N}\sum_{\mathbf{x}} u(\mathbf{x})^{\gamma} - 0.5 = 0$,	Simple. No parameters.	Poor enhancement in some images. Saturation of bright regions.

Earth observation satellites does not need the color. Indeed, in high-resolution optical satellites, such as Pleiades or WorldView, the resolution of the chromatic channels is four times smaller than the panchromatic one. It follows that the color images are obtained by *pansharpening*, which is the process wherein the high frequencies (and therefore the contrast) of the panchromatic channel is transferred to the chromatic channels. Thus, contrast perception depends on the panchromatic channel.

We discarded the use of quantitative measures in the evaluation of the algorithms because each of these measures capture only a certain aspect of the images' characteristics but is unable to assess their global quality. For instance, enhancement measure [13] measures the image entropy, and the histogram equalization (HE) algorithm (designed to maximize this entropy) gets good scores based on this measure. However, our tests show that the quality of the results of this algorithm is far from optimal.

This paper is organized as follows. In Section II, we describe and analyze the results obtained from the first study. From a far larger set of methods for global and local contrast enhancement, we selected 12 representative algorithms. These are described in Section II-A. We tested the algorithms on excerpts from a set of problematic satellite images, which were proposed by experts and obtained, from a broader set of experts, individual qualitative (subjective) evaluation of the results. The obtained score is analyzed in Section II-B, and intermediate conclusions are given in Section II-C. The second benchmark is surveyed in Section III. Section III-A describes the methods added in the second study. The results of the second benchmark are shown in Section III-B, where some preliminary conclusions are drawn. Interestingly, the methods that were best ranked in the initial benchmark (multiscale retinex family) are confirmed in the second benchmark. Qualitative results were compared and analyzed, and our conclusions are presented in Section IV.

II. FIRST STUDY

A. Methods for the First Study

In our preliminary study, we investigated the effectiveness of the state-of-the-art contrast enhancement methods in remote sensing and satellite images. Among the state-of-the-art contrast enhancement methods, we selected, for obvious operational reasons, the simplest and fastest algorithms. We picked the best methods in the three main distinct categories of enhancement algorithms: histogram modification methods, center/surround methods, and gradient-domain methods. The tested color images were encoded in RGB space. We denote them by $\vec{u} = (u_R, u_G, u_B)$, where u_R, u_G, and u_B are monochrome images that convey the information on the red, blue, and green chromatic channels, respectively. In what follows and without loss of generality, u shall refer to any of those monochrome images. The algorithms described in the following sections were applied independently on each color channel. Moreover, to avoid dependence on the image format (8-, 10-, or 12-bit images), we assume that the dynamic range of each channel is normalized to the interval [0, 1]. We shall denote by $I = (u_R + u_G + u_B)/3$ the gray intensity and by N the image size. Because photo interpreters are very conservative about modifying an image content, we shall consider the transforms of increasing complexity, which take more and more liberties with the original image.

1) Histogram-Based Methods: The histogram can be modified by means of functions which compress, translate, or expand the intensity gray levels. Histogram-based methods are image enhancement techniques operating directly on the pixel values. These image processing functions can be expressed by $g(\mathbf{x}) = T[u(\mathbf{x})]$, where $g(\mathbf{x})$ is the processed image at pixel $\mathbf{x} = (x, y)$ and T is a monotone function. The big advantage of such methods (which turns out to be also a limitation) is that isolevel sets of the image are maintained, and the order of image intensities is also preserved. The analyzed methods belonging to this category are briefly described in Table I.

2) Center/Surround Methods: The retinex theory developed by Land and McCann [16] is a strong incentive to go beyond histogram modifications and to allow distinct alterations to the colors of two pixels with the same initial color. This decision is based on the observation that the human perception of each pixel color in an image depends on its surrounding pixels. Thus, there is no use in keeping equal colors that can anyway be perceived as distinct or, conversely, in maintaining a numerical difference between colors that are anyway perceived as equal. Land and McCann established that the visual system does not perceive an absolute lightness but rather a relative lightness, namely, the variations of lightness in local image regions. In their first work [16], they proposed a complex algorithm involving image paths to compute the relative lightness. Many

TABLE II
CENTER/SURROUND METHODS

Name	Description	Advantages	Disadvantages
Multi-Scale Retinex (MSR, [25])	$T_{MSR}(u(\mathbf{x})) = \sum_{k=1}^{K} w_k \left[\log u(\mathbf{x}) - \right.$ $\left. - \log((G_{\sigma_k} * u)(\mathbf{x}))\right]$, $G_{\sigma_k}(\mathbf{x}) = C_k \exp[-(\|\mathbf{x}\|^2)/2\sigma_k^2]$	Well-known and very used method. In general, good results.	Arbitrary bounds in the solution. Possible halo effects. Excessive parameters. Parameters: K, ω_k and σ_k, for every k.
Other retinex kernels [22]	$T_{Rkernel}(u(\mathbf{x})) =$ $\log(u(\mathbf{x})) - \log((u * F)(\mathbf{x}))$		
Land Kernel (MSRKLAND)	$F_{\text{land}}(\mathbf{x}) = \frac{1}{\|\mathbf{x}\|^2}$	Scale invariant, faithful to the original method. No parameters.	Is not integrable. Possible halo effects. Saturation of bright zones.
ACE Kernel (MSRKACE)	$F_{\text{ACE}}(\mathbf{x}) = \frac{1}{\|\mathbf{x}\|}$	No parameters. Good color rendition.	Is not integrable. Possible halo effects.
New Kernel (MSRNK)	$F_{\text{new}}(\mathbf{x}) = C\frac{G_{\sigma_2}(\mathbf{x}) - G_{\sigma_1}(\mathbf{x})}{\|\mathbf{x}\|^2}$, $\|\mathbf{x}\| \neq 0$ $F_{\text{new}}(\mathbf{x}) = C\frac{\sigma_1^{-2} - \sigma_2^{-2}}{2}$, $\|\mathbf{x}\| = 0$ $\sigma_i = a^{s_i}$, $i = 1, 2$	Integrable. The parameters allow to adjust the level of contrast.	Possible halo effects. Parameters: s_1, s_2 and a.
Local Color Correction (LCC, [23])	$T_{LCC}(u(\mathbf{x})) = (u(\mathbf{x}))^{2^{\frac{0.5 - M(\mathbf{x})}{0.5}}}$, $M(\mathbf{x}) = (G_r * (1 - I))(\mathbf{x})$.	Allows simultaneous shadow and highlight adjustment.	Possible halo effects. Parameter: r.
Automatic Color Enhancement (ACE, [24])	$T_{ACE}(u(\mathbf{x})) = \frac{R(\mathbf{x}) - R_{min}}{R_{max} - R_{min}}$, $R(\mathbf{x}) = \sum_{\mathbf{y} \in \Omega - \mathbf{x}} \frac{s_\alpha(u(\mathbf{x}) - u(\mathbf{y}))}{\|\mathbf{x} - \mathbf{y}\|}$, $s_\alpha(t) = \min(\max(\alpha t, -1), 1)$, $\alpha > 1$.	The enhancement process is consistent with perception. Local method.	Excessive enhancement for certain values of the parameter. Parameter: α.

TABLE III
GRADIENT-DOMAIN METHODS

Name	Description	Advantages	Disadvantages
Global contrast enhancement (SCE_global, [27])	$\mathbf{V} = \lvert\nabla u\rvert^{\alpha - 1}\nabla u$	Global method.	Poor enhancement in some images. Parameter: α.
Selective contrast enhancement (SCE_dark, [28])	$\mathbf{V} = \begin{cases} a\nabla u & \text{in } D \\ \nabla u & \text{otherwise} \end{cases}$, $D = \{\mathbf{x} \in \Omega;\ I(\mathbf{x}) \leq T\}$	Well adapted to images with back light or strong shadows. Reveals details in shadows.	"Manual" selection of the dark zone. Parameters: a and T.

different implementations and interpretations have followed this first work, i.e., [16]–[19] to name a few.

In a posterior work, Land [20] published an alternative to the initial path-based algorithm. This new implementation proposes to compute the lightness as the logarithm of the ratio between the value in a pixel and the average value of the surround, considering this surround with a density that is proportional to the inverse of the square distance. This center/surround operation is a sort of nonlinear high-pass filter defined by

$$L(\mathbf{x}) = \log\left(u(\mathbf{x})\right) - \log\left(\langle u(\mathbf{y})\rangle_w\right) \tag{1}$$

where $\langle\rangle_w$ denotes the weighted average, which is the convolution of the image u with a radial kernel w. In this category, we considered the most classic center/surround algorithm in the literature, namely, NASA's multiscale retinex, as proposed by Jobson *et al.* [21] who used a Gaussian kernel for the surround. Moreover, we explored three alternative kernels for the surround [22]: the Land kernel, which is the inverse of the squared distance; the ACE kernel, which is the inverse of the distance; and finally, a new kernel that finds an acceptable compromise between scale invariance and integrability. This new kernel is the result of combining all the Gaussians from an initial scale σ_1 to a final scale σ_2, which is integrable and, in the limit case, tends to the Land kernel, which is the only one to be scale invariant [22]. Low color correction (LCC) [23] and the original ACE [24] are also clearly center/surround methods. These methods are briefly explained in Table II.

3) Gradient-Domain Methods: Poisson image editing [26] is a technique to reconstruct the image from a *guidance vector field* $\mathbf{V}$. Then, the problem is to minimize

$$\min_g \int_\Omega |\nabla g - \mathbf{V}|^2. \tag{2}$$

The minimizer is uniquely determined by the Euler–Lagrange equation $\Delta g = \operatorname{div}\mathbf{V}$, over Ω, with homogeneous Neumann boundary condition $\partial g/\partial \mathbf{n} = 0$ over $\partial\Omega$, where $\mathbf{n}$ is the outward normal vector to the boundary. The Poisson equation can be efficiently performed by fast Fourier transform.

In this category, we consider an algorithm applying this technique, where the gradient vector field of the image is modified. The proposed transformation is $T_{\text{SCE}}(u(\mathbf{x})) = g(\mathbf{x})$, where g is the solution of (2).

We have analyzed two different variants. The first variant enhances all small gradients in the image by means of a power function. The second variant enhances the contrast by increasing the gradient in the dark regions of the image. These two variants are briefly detailed in Table III.

B. Qualitative Evaluation of Results From the First Study

This section summarizes the results of the evaluation of the methods described in the earlier section by 27 experts on

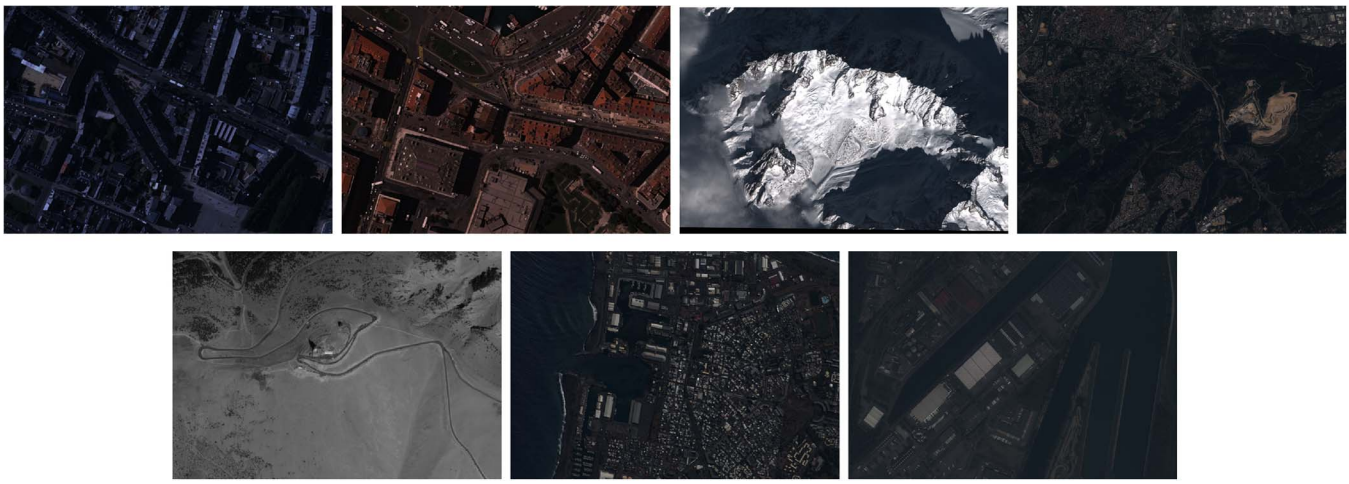

Fig. 3. Input satellite images used in the tests. (Left to Right, Top to Bottom) Amiens, Marseille (30-cm image simulation, CNES 2014), Argentiere, Calanques, Ventoux (distribution Airbus DS/Spot Image, CNES 2013), Saint Paul, and Strasbourg (distribution Airbus DS/Spot Image CNES 2012).

satellite image analysis [nine experts from the French Space Agency (CNES)] and image processing (13 researchers from CMLA[1] and five from UIB[2]).

Each expert was given the address of the online facility[3] displaying seven large images and was allowed to select subimages of size 1000×500. This size was chosen to fit in any computer screen and leave enough space to display the rating command panel. No time limit was given to the experts, and they could make as many selections as they wished. No guideline was given to the experts as to their rating criteria. Fig. 3 displays the seven images that were used in the tests (provided by CNES). Five of them are from Pleiades satellites and two are from the simulations[4] (Amiens and Marseille). For each chosen excerpt, the results of the 12 algorithms were displayed, and the experts had to rate them all.

The input images and the results were in 12-bit integer format. In order to display the results, the input image and the processed images were converted to 8 bits by the following linear transformation, applied independently on each color channel: displayed value $=$ (input value $-\min$)$/(\max - \min) \times 255$, where $\max$ and $\min$ are, respectively, the maximum and minimum values of the 12-bit image over all the channels.

In each experiment, the expert had to assess the quality of each displayed result by assigning to it a value of $+1$ (good), -1 (bad), or 0 (indifferent). The default value being 0, the experts could leave this value unchanged. The votes for the methods were assigned blindly since the user did not know which result corresponds to which method. The selected subimage, generally dark, was drastically transformed by stretching its dynamics. Thus, it was not obvious for the users to figure out which of the images was the input one. The tested methods and their corresponding acronyms are summarized in Table IV. The default (fixed) parameters of the methods (see Section II for details) are also listed in the table. The parameters for every method have been evaluated independently by four experts and are fixed, with a strong agreement between them that these values gave the best compromise between the enhancement of the dark and bright parts on the benchmark images.

TABLE IV
LIST OF TESTED METHODS AND DEFAULT PARAMETERS

Acronym	Algorithm	Parameters
ORIGINAL	The linearly intensity transformed version of the input image	
IG	Ideal Gamma	
LCC	Local Color Correction	$r = 5\%$ image width
SCB	Simplest Color Balance	$s_1 = s_2 = 0.5$
HE	Histogram Equalization	
PE	Piecewise Linear Equalization	$N = 3$, smin=0.5, smax=3
SCE_global	Selective Contrast Enhancement (global version)	$\alpha = 0.8$
SCE_dark	Selective Contrast Enhancement ('dark' version)	$T = 50, a = 3$
MSR	Multi-Scale Retinex	low scale=15, medium scale=80, high scale=250
MSRKLAND	Kernel Retinex, Land-type kernel	
MSRKACE	Kernel Retinex, ACE-type kernel	
MSRNK	Kernel Retinex, new kernel	$s_1 = 0$, $s_2 = 10$, $a = 4$
ACE	Automatic Color Enhancement	$\alpha = 5$

Fig. 4 summarizes the 235 experiments performed by the different groups of experts over a period of two months (from November 7, 2014 to January 13, 2015). The CNES experts performed 92 experiments, the UIB experts performed 81 experiments, and the CMLA experts performed 62 experiments. The graphic shows the number of positive, negative, and zero votes for each method, as well as the net value of the votes (positives minus negatives). The results are sorted by decreasing net value.

Fig. 5 displays some examples of the results of the methods with global best scores on two subimages. For comparison, the results of one of the worst ranked methods (HE) are also displayed.

[1]CMLA: Centre de Mathématiques et de leurs Applications, ENS Cachan, France.

[2]UIB: Universitat de les Illes Balears, Spain.

[3]http://dev.ipol.im/lisani/ipol_demo/workshop_colorsat_ranking_v1/

[4]Aerial images with 30-cm resolution.

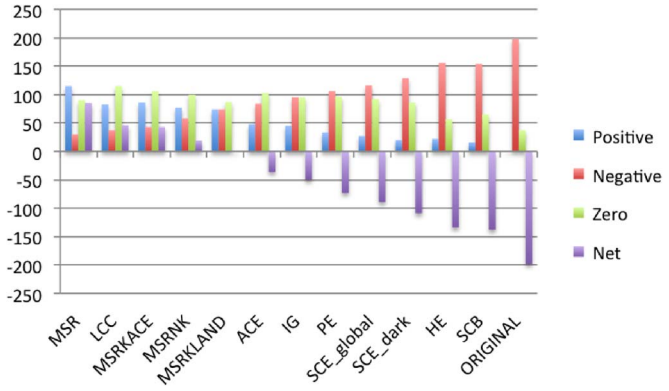

Fig. 4. Global results of voting for the first benchmark.

C. Conclusions from the First Study

- Globally, the best methods are (from best to worst) MSR, LCC, MSRKACE, MSRNK, and MSRKLAND. The rest of the methods have negative net values.
- None of the global techniques (HE, PE, SCB, and IG) gets positive net votes. The reason given afterwards by the experts is that all of these methods tend to saturate the bright zones (as can be observed in Fig. 5).
- The performance of each method depends on the image on which it is applied. For instance, for the image in Fig. 5 right column, LCC got better scores than MSR, whereas for the one in Fig. 5 left column, it was the opposite. In general, it seems that MSR gets positive net results for all the images, whereas LCC and MSRKACE get negative net results in some cases.
- The votes of each user might be based on different subimages. A better measure of the performance of each method could perhaps have been obtained by testing them on the same subimages. However, the advantage of leaving the choice of the subimage to experts was to leave them free to choose the most problematic image parts.
- In general, the results of the various methods are uncorrelated, which means that one cannot predict the results of one method from the results on a different method. Table V shows the correlations between the different methods. In general, LCC is highly uncorrelated from the other methods, MSR exhibits a very slight correlation with MSRKACE, MSRKLAND, and MSRNK, MSRKACE and MSRNK are uncorrelated, and MSRKLAND and MSRNK are quite correlated.

Perhaps, the most striking outcome of this paper is that the displayed input image *never* obtained a positive vote. It obtained 198 negative votes and only 37 neutral votes. This means that experts massively preferred contrast adjustment methods, and among them the most sophisticated ones, of the retinex type. It is important to notice that as the experts ignored what the input image was, they could only rate the image quality, regardless of any fidelity criterion to some ground truth. In this context, it appears that they genuinely preferred to give up the physically faithful image for the most readable image. It is also noticeable that an image readability criterion seems to have dominated aesthetic criteria, which might, for instance,

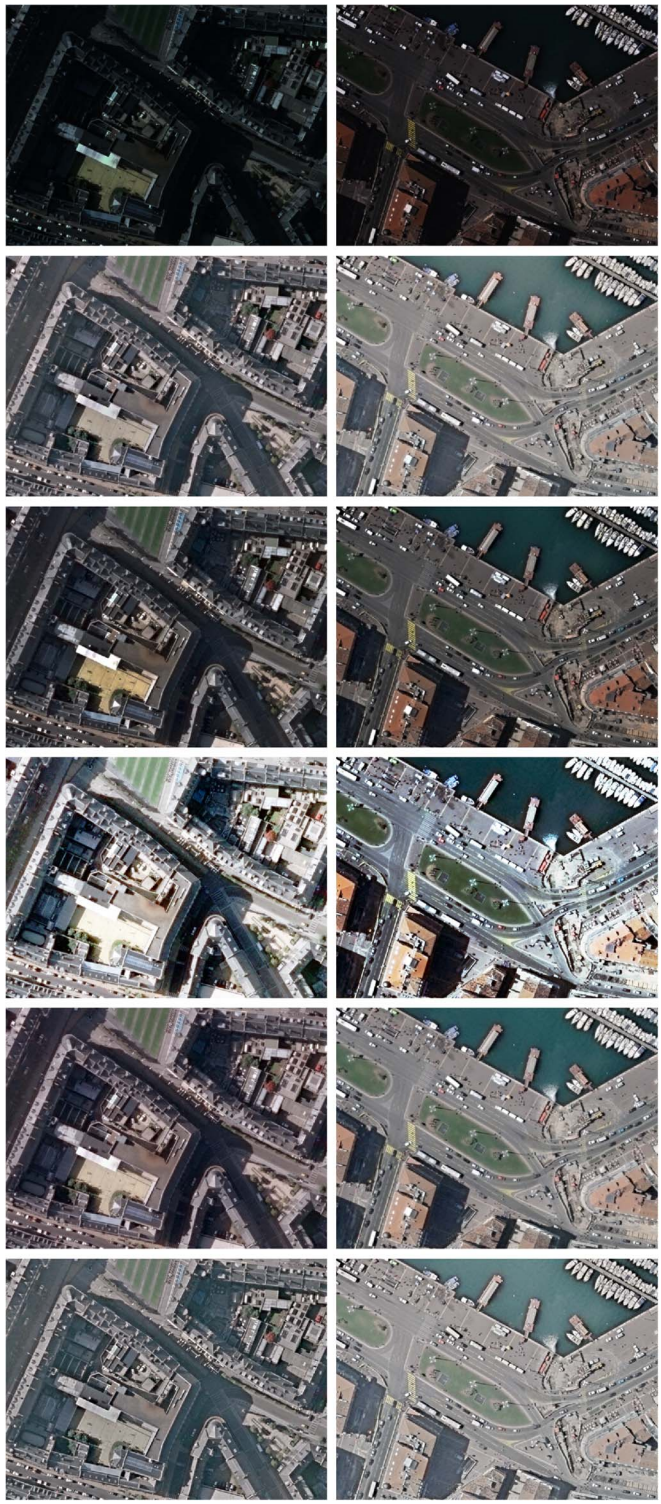

Fig. 5. Example results of the methods with global best scores for the excerpts of the first two images in the first row of Fig. 3. (Left Column) Amiens image. (Right column) Marseille image. (Top to Bottom) Original subimages and the results of MSR, LCC, HE, MSRKACE, and MSRNK. The result of HE, one of the worst ranked methods, is displayed for comparison.

TABLE V
CORRELATION COEFFICIENTS BETWEEN THE TOP FIVE METHODS

	MSR	MSRKLAND	MSRNK	MSRKACE
LCC	-0.08	-0.17	-0.27	0.16
MSR		0.46	0.57	0.48
MSRKLAND			0.77	0.11
MSRNK				0.18

TABLE VI
TONE-MAPPING METHODS

Name	Description	Fixed Parameters
Drago et al. 2003 (Drago03, [32])	The method is based on logarithmic compression of luminance values, imitating the human response to light. A bias power function is introduced to adaptively vary logarithmic bases,	Gamma coefficient: $\gamma = 1.7$ Bias parameter: $b = 0.85$
Durand and Dorsey 2002 (Durand02, [33])	This method is based on a two-scale decomposition of the image into a base layer, encoding large-scale variations, and a detail layer. The base layer is obtained using the bilateral filter	Size of the spatial kernel $\sigma_s = 40$ Size of the channel level $\sigma_r = 0.4$ $\gamma = 3$
Fattal et al. 2002 (Fattal02, [34])	The method computes a Gaussian pyramid. Gradients of larger magnitude are attenuated. The image is then reconstructed by classic Poisson editing.	Threshold gradient value α=1 Strength of gradient modification $\beta = 0.9$ Amount of saturation $s = 0.8$
Reinhard and Devlin 2005 (Reinhard05, [35])	The algorithm is a γ correction inspired by physiology. The methods is based on a variant of the Naka and Rushton equation, and statistical global measurements of the image.	Brightness adaptation $f' = 0$ Chromatic adaptation $c = 0$ Lightness adaptation $a = 1$
Mai et al. 2011 (TMM, [36])	A statistical model that approximates the distortion resulting from the combined processes of tone-mapping and compression. Method very similar to PE with less parameters.	Number of bins $N = 40$ Inverse of the power s_k $\gamma = 3$ Min. and max. slope $s_{min} = 0$, $s_{max} = 200$

prefer a stronger global contrast to the sharp local contrast given by retinex methods. These methods make the image aspect not only more visible but also more uniform and with a loss of hue contrast, as shown in Fig. 5.

III. SECOND BENCHMARK

Our first exploratory study provided interesting and clear cut conclusions, but led us and the experts to a series of unforeseen objections, questions, and suggestions. Their common object was to tighten the decision method and the selection criteria. The main questions left unanswered were as follows.

- The fact that each expert selected a different set of subimages for the evaluation prevented the generalization of the conclusions. Thus, in the second study, the set of images was fixed to nine excerpts of larger images. These excerpts were selected following the recommendations in [12]. The images were categorized in landscape or nature images and urban or coastal images, and different excerpts were selected taking into account these categories and the "ness" image quality of the images.
- In the first study, we observed that experts declared to take into account mainly two factors, namely, the contrast (visibility in dark zones) and the no-saturation (visibility in bright zones). Thus, in the second study, the experts were asked to assess separately these two factors on each image. Experts were asked to rate each factor as -1, 0, or 1, depending on whether it was of bad, poor, or good quality, respectively.
- Finally, we decided to separate the study of contrast enhancement from that of color enhancement by using only grayscale images in the benchmark. This is due to the fact that color information can mask contrast and saturation information, and a more reliable assessment of the contrast enhancement can be made on a grayscale image.
- Recent tone-mapping methods developed in the realm of new high-dynamic-range (HDR) imaging techniques had not been included in the comparison. We selected five of the best tone-mapping methods for the extended benchmark. These methods were added to the four methods with better scores in the first study.
- These experts were informed that some of the algorithms preserve the intensity consistency, whereas the others did not. None of the experts considered it a major issue for two reasons: 1) because they knew that the linearly stretched input image was present in the comparison set; and 2) because they were aware of the retinex theory and know that human perception drastically alters the intensity consistency. In fact, the original images were ranked last.

TABLE VII
METHODS EVALUATED IN THE BENCHMARK

Acronym	Method
ORIGINAL	The linearly intensity transformed version of the input image
LCC	Local Color Correction (Section II-A)
MSR	Multi-Scale Retinex (Section II-A)
MSRKACE	Multi-Scale Retinex with ACE Kernel (Section II-A)
MSRNK	Multi-Scale Retinex with New Kernel (Section II-A)
DRAGO03	Drago Tone Mapping Method (Section III-A)
DURAND02	Durand Tone Mapping Method (Section III-A)
FATTAL02	Fattal Tone Mapping Method (Section III-A)
REINHARD05	Reinhard Tone Mapping Method (Section III-A)
TMM	Mai Tone Mapping Method (Section III-A)

In the succeeding sections, we detail the considered tone-mapping methods and the obtained results of this second study.

A. Added Methods in the Second Study

The goal in tone mapping is to reproduce a faithful representation of an HDR scene on a low-dynamic-range display device. A review of the state-of-the art tone reproduction can be found in [29], and a more complete study on tone-mapping and HDR imaging can be found in [30].

For our second study, we used the pfstmo package (tone-mapping operators) [31], which contains the implementation

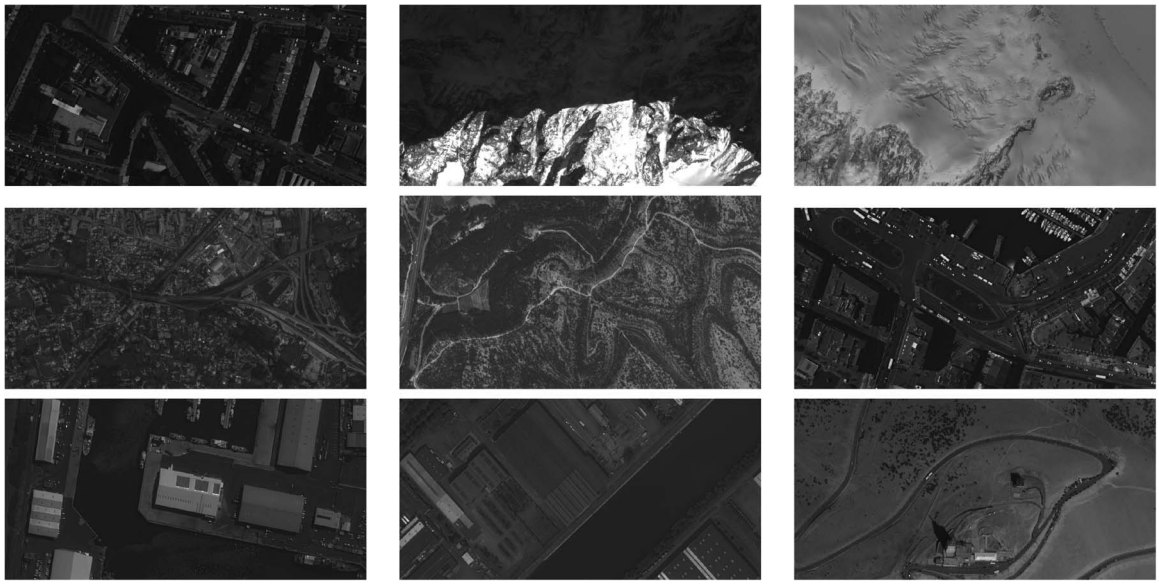

Fig. 6. Input images used in the demo for the second benchmark. (Left to Right, Top to Bottom) Amiens, Argentière 1, Argentière 2, Calanques 1, Calanques 2, Marseille, Saint Paul, Strasbourg 1, and Ventoux.

of state-of-the-art tone-mapping operators. The implemented methods were studied and analyzed, mainly for their behavior when varying their parameters. The selected methods are summarized in Table VI. The parameters for every method have been evaluated independently by four experts and are fixed, with a strong agreement between them that these values gave the best compromise between enhancement of the dark and bright parts on the benchmark images. The fixed values are indicated in the table.

B. Second Benchmark Results

The users were asked to evaluate the performance of several enhancement methods (see Table VII) on the images displayed in Fig. 6. These images are excerpts of larger images. Amiens and Marseille images are 30-cm simulations, and the rest are spot images. The input color images were converted to grayscale by averaging the three color channels.

The online demo[5] used to evaluate the methods worked as follows.

1) The user selected an input image from the set of nine possible choices.
2) The demo displayed ten images: the input image and the results of the nine methods under evaluation. The images were unlabeled, which means that the user did not know which image corresponded to which method and ignored which of them was the input image.
3) The user had to evaluate the images with respect to two quality features (contrast and saturation, see succeeding discussion) and assigned a vote (positive, negative, or zero) to each feature. Since the correspondence image method was unknown, this resulted in a blind voting over the methods.

[5]http://dev.ipol.im/lisani/ipol_demo/workshop_ranking_selected_gray/

TABLE VIII
NET VOTES OF THE SECOND BENCHMARK FOR EACH GROUP OF USERS

		Original	LCC	MSR	MSRKACE	MSRNK	Drago03	Durand02	Fattal02	Reinhard05	TMM
CONTRAST	SERTIT	-49	-5	35	21	10	2	-11	-5	-36	24
	CNES	-17	-3	14	0	6	-2	-1	10	-13	2
	CMLA	-37	-4	16	21	10	-4	0	12	-30	14
	UIB	-23	3	15	11	15	6	8	18	-18	5
SATURATION	SERTIT	-12	-9	-1	8	20	-8	12	-4	-26	-18
	CNES	1	-4	3	3	3	-6	2	1	-8	-7
	CMLA	2	2	7	7	3	-5	2	0	-12	-13
	UIB	11	-1	-1	2	13	-2	10	3	-8	-12

The experts were asked to rate all the methods for two features.

- *Contrast*: This feature shows the visibility in dark zones of the images. According to this criterion, the users were asked to assign a positive vote to the images exhibiting good visibility in dark regions, a negative vote to images with poor visibility in dark regions, and a zero vote to images without a remarkable good or bad visibility in dark regions.
- *Saturation*: This feature assesses the visibility in bright zones of the images. According to this criterion, the users were asked to assign a positive vote to the images exhibiting good visibility (i.e., no saturation) in bright regions, a negative vote to images with poor visibility (i.e., saturation) in bright regions, and a zero vote to images without a remarkable good or bad visibility in bright regions.

Different experts were asked to cast their votes. The selected experts belong to four different groups in Europe. The number of votes was as follows: 22 votes of the satellite image quality experts at CNES, 48 votes of image processing experts at CMLA, 27 votes of image processing experts at UIB, and

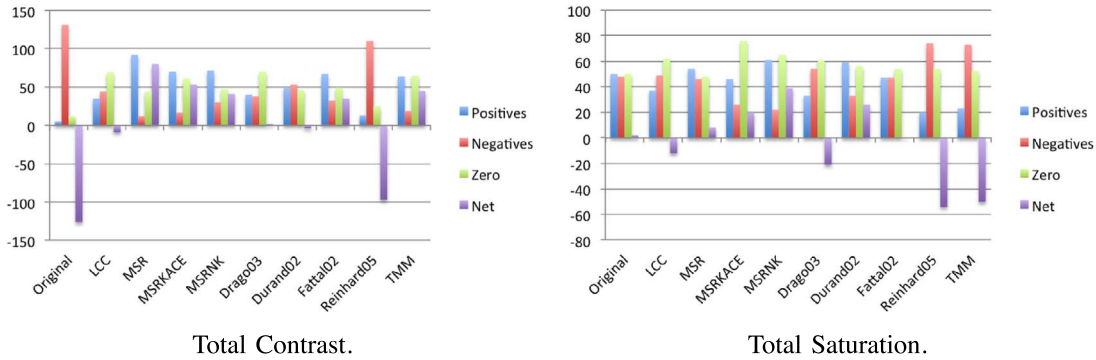

Total Contrast. Total Saturation.

Fig. 7. Total voting results.

TABLE IX
MEAN AND STANDARD DEVIATION OF NET VOTES ACROSS THE IMAGES

		Original	LCC	MSR	MSRKACE	MSRNK	Drago03	Durand02	Fattal02	Reinhard05	TMM
CONTRAST	Mean	-13.3	-1.2	8.4	5.4	4.8	-0.1	0.2	3.8	-10.1	4.9
	Std	5.2	3.4	3.9	3.7	3.9	4	8.1	2.3	6.7	3.1
SATURATION	Mean	0.9	-1.2	0.9	2.3	4.2	-1.7	2.4	-0.6	-5.3	-5.2
	Std	4.6	5.6	5.4	3.6	3.3	5.6	4.9	4.6	5.1	4.9

51 votes of photo interpreters skilled in emergency cartography of satellite images at the Service Régional de Traitement d'Image de Téleédétection (SERTIT). The visual setup was unified by being displayed in the same HTML pages for all users. These experts were invited to display these pages in the most favorable light environment (best angle of view, best screen contrast on 8-bit displays, and diffused day light). Contrary to usual psychophysical experiments with naive subjects, we had to trust the expertise of the subjects to define their own best visualization conditions. Indeed, this is how they will use the images.

The results of the voting are summarized in Table VIII. This table shows, for each group of users and for each feature under study, the net votes (positive minus negatives) of each method. The cumulated votes from all the groups are displayed in Fig. 7. In order to assess the stability of the results with respect to the images' content, we have also computed the mean and standard deviation of the net votes of each method across the images. The results are shown in Table IX.

The analysis of the voting results permits to draw the following conclusions.

- The top-ranked methods in terms of contrast enhancement are (sorted by decreasing net total value): MSR, MSRKACE, TMM, MSRNK, and Fattal. The rest of the methods obtain a negative or zero net value.
- The global results are not always consistent with the results from the different groups of users. For instance, Fattal obtains the best score by the UIB group and the second best by the CNES group but a negative net vote by the SERTIT group; MSR is considered the best method by CNES and SERTIT groups, whereas it is the second best for CMLA and UIB groups; MSRACE obtains a zero net value by the CNES group, but it is considered among the best methods by the rest of groups.
- In terms of saturation, the best methods are (again sorted by decreasing net total value): MSRNK, Durand, MSRKACE, and MSR. The rest of the methods obtain a negative or zero net value.
- The global results in terms of saturation are, again, not always consistent with the results from the different groups. For instance, MSR obtains negative (but small) net values by UIB and SERTIT but positive values by CMLA and CNES.
- It must be remarked that the total net value of the input image, in terms of saturation, is positive (but small). This means that most users consider that the visualization of bright zones is already good in the input image even if, in terms of visualization of dark zones, the input image obtains the worst score.
- In global terms, the only methods that obtain total positive net votes are the three multiscale retinex methods: MSR, MSRKACE, and MSRNK.
- MSRNK is the only method to get positive net values by all the groups in both categories. MSRKACE also obtains nonnegative net votes by all the groups (it obtains a zero net vote on contrast by CNES).
- If we focus on the negative votes, in the contrast case, we can observe that the methods with fewest negative votes are MSR, MSRKACE, TMM, and MSRNK, in this order. In the saturation case, the methods with fewest negative votes are MSRNK, MSRKACE, Durand02, and MSR. Then, we conclude that the multiscale retinex methods are the methods with fewest negative votes in both cases.
- Concerning the stability of the results with respect to the image content, the high values of mean and the small values of standard deviation shown in Table IX for MSRNK and MSRKACE confirm that these methods provide the best performances both in terms of contrast and saturation for all the images.

Fig. 8 displays the results obtained by the best methods in each category for two images.

IV. CONCLUSION AND FUTURE WORK

We have reviewed in this paper some of the most representative algorithms on contrast enhancement and tone mapping in the literature, and we have tested them in the specific case of satellite images. In order to evaluate the results, we have

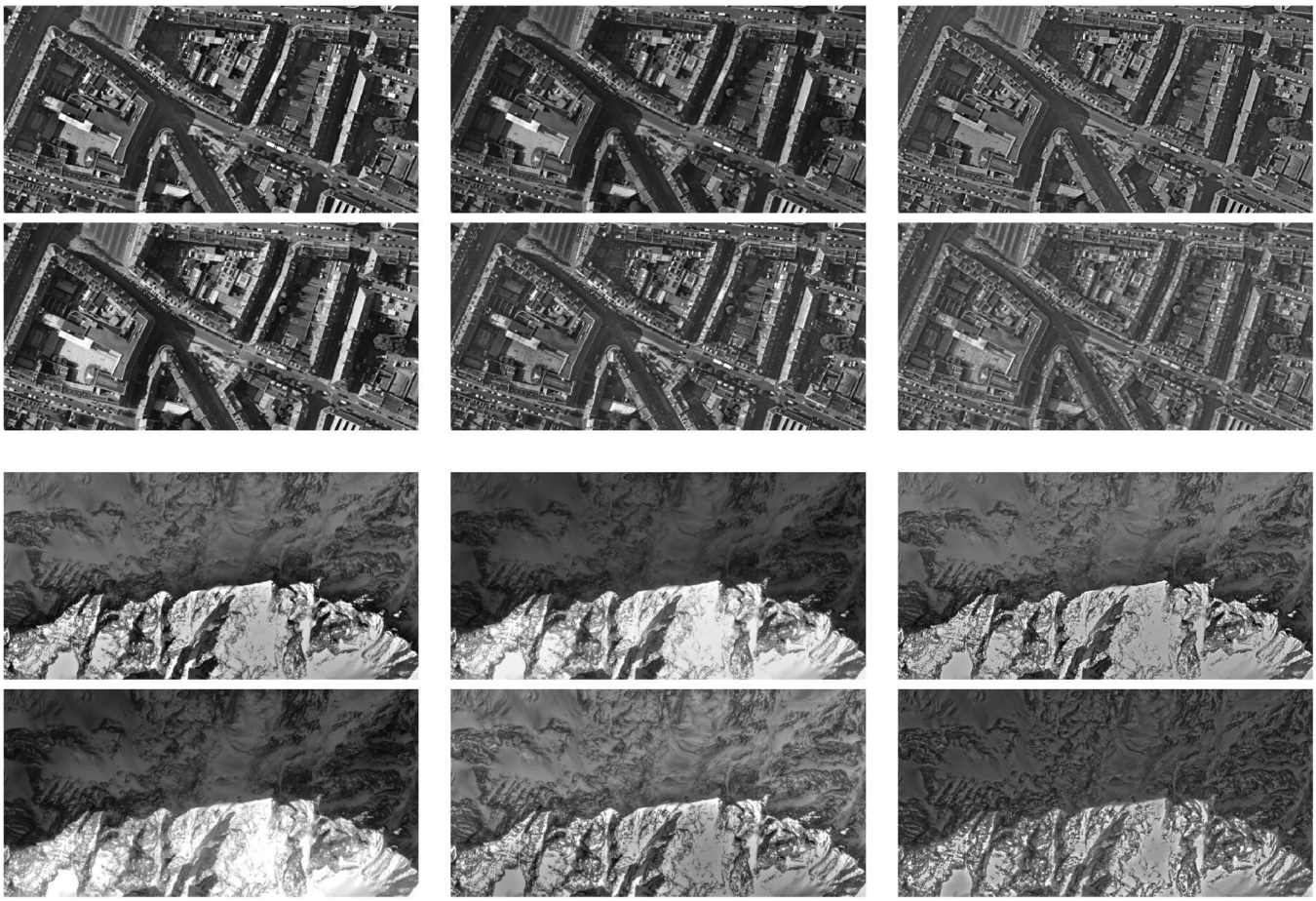

Fig. 8. Results of the top-ranked methods in terms of contrast improvement and saturation control. (First and second rows) Results for image Amiens (see first image in first row of Fig. 6). (Third and fourth rows) Results for image Argentière 1 (see second image in first row of Fig. 6). For each set of results, (Left to Right, Top to Bottom) MSR (1, 4), MSRKACE (2, 3), MSRNK (4, 1), TMM (3, ×), FATTAL02 (5, ×), DURAND02 (×, 2). The two numbers after the method name indicate the position of the method in the sorted ranking (decreasing order) of net votes, for both contrast (left value) and saturation (right value). × means that the method got a negative score.

performed a qualitative rating with the help of a group of experts, in two stages. We found that local techniques of the retinex family got the best scores in terms of visual quality. The qualitative results suggest that the best enhancement method is the multiscale retinex with a new kernel.

Although, in our first benchmark color, images were used, in the second stage of the study, we decided to focus on the enhancement of the image brightness. This simplified the assessment of the algorithms since experts could focus on just two factors (visibility in dark and bright regions), without taking into account the color quality. Color is nevertheless an important subsidiary quality criterion, and we plan to incorporate it in a future benchmark. Indeed, it remains to select the best method to incorporate the original color information to the enhanced brightness image.

ACKNOWLEDGMENT

The authors would like to thank the experts from CNES, CMLA, SERTIT, and UIB for their collaboration. The authors would also like to thank CNES for providing the satellite images.

REFERENCES

[1] J. B. Campbell, *Introduction to Remote Sensing*, 2nd ed. New York, NY, USA: Taylor & Francis, 1996.

[2] J. R. Schott, *Remote Sensing: The Image Chain Approach*. London, U.K.: Oxford Univ. Press, 1997.

[3] R. A. Schowengerdt, *Remote Sensing: Models and Methods for Image Processing*, 2nd ed. New York, NY, USA: Academic, 1997.

[4] P. Lier, C. Valorge, and X. Briottet, *Imagerie Spatiale*. Toulouse, France: Cépaduès-Editions, 2008.

[5] H. Li, L. Zhang, and H. Shen, "A perceptually inspired variational method for the uneven intensity correction of remote sensing images," *IEEE Trans. Geosci. Remote Sens.*, vol. 50, no. 8, pp. 3053–3065, Aug. 2012.

[6] J. Liu *et al.*, "Illumination and contrast balancing for remote sensing images," *Remote Sens.*, vol. 6, no. 2, pp. 1102–1123, 2014. [Online]. Available: http://www.mdpi.com/2072-4292/6/2/1102

[7] J. H. Jang, S. D. Kim, and J. B. Ra, "Enhancement of optical remote sensing images by subband-decomposed multiscale retinex with hybrid intensity transfer function," *IEEE Geosci. Remote Sens. Lett.*, vol. 8, no. 5, pp. 983–987, Sep. 2011.

[8] E. Lee, S. Kim, W. Kang, D. Seo, and J. Paik, "Contrast enhancement using dominant brightness level analysis and adaptive intensity transformation for remote sensing images," *IEEE Geosci. Remote Sens. Lett.*, vol. 10, no. 1, pp. 62–66, Jan. 2013.

[9] J. Kuang, H. Yamaguchi, G. M. Johnson, and M. D. Fairchild, "Testing HDR image rendering algorithms," in *Proc. Color Imaging Conf. Soc. Imaging Sci. Technol.*, 2004, pp. 315–320.

[10] J. McCann and A. Rizzi, *The Art and Science of HDR Imaging*. New York, NY, USA: Wiley, 2012.

[11] M. Lambers, H. Nies, and A. Kolb, "Interactive dynamic range reduction for SAR images," *IEEE Geosci. Remote Sens. Lett.*, vol. 5, no. 3, pp. 507–511, Jul. 2008.
[12] P. G. Engeldrum, "Psychometric scaling: Avoiding the pitfalls and hazards," in *Proc. PICS*, 2001, pp. 101–107.
[13] S. S. Agaian, B. Silver, and K. A. Panetta, "Transform coefficient histogram-based image enhancement algorithms using contrast entropy," *IEEE Trans. Image Process.*, vol. 16, no. 3, pp. 741–758, Mar. 2007. [Online]. Available: http://dx.doi.org/10.1109/TIP.2006.888338
[14] N. Limare, J.-L. Lisani, J.-M. Morel, A. B. Petro, and C. Sbert, "Simplest color balance," *Image Process. On Line*, vol. 1, pp. 716–725, 2011.
[15] J.-L. Lisani, A.-B. Petro, and C. Sbert, "Color and contrast enhancement by controlled piecewise affine histogram equalization," *Image Process. On Line*, vol. 2, pp. 243–265, 2012.
[16] E. Land and J. McCann, "Lightness and retinex theory," *J. Opt. Soc. Amer.*, vol. 61, no. 1, pp. 1–11, Jan. 1971, doi: 10.1364/JOSA.61.000001.
[17] J. Morel, A. B. Petro, and C. Sbert, "A PDE formalization of the retinex theory," *IEEE Trans. Image Process.*, vol. 19, no. 11, pp. 2825–2837, Nov. 2010.
[18] N. Limare, A. B. Petro, C. Sbert, and J.-M. Morel, "Retinex Poisson equation: A model for color perception," *Image Process. On Line*, vol. 1, pp. 1–12, 2011.
[19] B. K. P. Horn, "Determining lightness from an image," *Comput. Graph. Image Process.*, vol. 3, pp. 277–299, 1974.
[20] E. Land, "An alternative technique for the computation of the designator in the retinex theory of color vision," *Proc. Nat. Acad. Sci.*, vol. 83, no. 10, pp. 3078–3080, 1986.
[21] D. Jobson, Z. Rahman, and G. Woodell, "A multiscale retinex for bridging the gap between color images and the human observation of scenes," *IEEE Trans. Image Process.*, vol. 6, no. 7, pp. 965–976, Jul. 1997, doi: 10.1109/83.597272.
[22] J. Morel, A. B. Petro, and C. Sbert, "What is the right center/surround for retinex?" in *Proc. ICIP*, 2014, pp. 4552–4556.
[23] A. Moore, J. Allman, and R. M. Goodman, "A real-time neural system for color constancy," *IEEE Trans. Neural Netw.*, vol. 2, no. 2, pp. 237–246, Mar. 1991.
[24] A. Rizzi, C. Gatta, and D. Marini, "A new algorithm for unsupervised global and local color correction," *Pattern Recognit. Lett.*, vol. 24, no. 1, pp. 1663–1677, 2003.
[25] A. B. Petro, C. Sbert, and J.-M. Morel, "Multiscale retinex," *Image Process. On Line*, vol. 4, pp. 71–88, 2014.
[26] P. Perez, M. Gangnet, and A. Blake, "Poisson image editing," *ACM Trans. Graph.*, vol. 22, no. 3, pp. 313–318, Jul. 2007.
[27] A. B. Petro and C. Sbert, "Selective contrast adjustment by Poisson equation," *Image Process. On Line*, vol. 3, pp. 208–222, 2013.
[28] J. M. Morel, A. B. Petro, and C. Sbert, "Fourier implementation of Poisson image editing," *Pattern Recognit. Lett.*, vol. 33, no. 3, pp. 342–348, Feb. 2012.
[29] K. Devlin, A. Chalmers, A. Wilkie, and W. Purgathofer, "Star: Tone reproduction and physically based spectral rendering," in *State of the Art Reports, Eurographics 2002*, D. Fellner and R. Scopignio, Eds. Geneva, Switzerland: Eurographics Association, Sep. 2002, pp. 101–123.
[30] E. Reinhard, G. Ward, S. Pattanaik, and P. Debevec, *High Dynamic Range Imaging: Acquisition, Display, and Image-based Lighting*. San Mateo, CA, USA: Morgan Kaufmann, 2005.
[31] G. Krawczyk, Pfstmo: Tone Mapping Library, accessed: Jun. 15, 2015. [Online]. Available: http://pfstools.sourceforge.net/pfstmo.html
[32] F. Drago, K. Myszkowski, T. Annen, and N. Chiba, "Adaptive logarithmic mapping for displaying high contrast scenes," *Comput. Graph. Forum*, vol. 22, no. 3, pp. 419–426, 2003.
[33] F. Durand and J. Dorsey, "Fast bilateral filtering for the display of high-dynamic-range images," *ACM Trans. Graph.*, vol. 21, no. 3, pp. 257–266, 2002.
[34] R. Fattal, D. Lischinski, and M. Werman, "Gradient domain high dynamic range compression," *ACM Trans. Graph.*, vol. 21, no. 3, pp. 249–256, 2002.
[35] E. Reinhard and K. Devlin, "Dynamic range reduction inspired by photoreceptor physiology," *IEEE Trans. Vis. Comput. Graph.*, vol. 11, no. 1, pp. 13–24, Jan./Feb. 2005.
[36] Z. Mai, H. Mansour, R. Mantiuk, P. Nasiopoulos, R. Ward, and W. Heidrich, "Optimizing a tone curve for backward-compatible high dynamic range image and video compression," *IEEE Trans. Image Process.*, vol. 20, no. 6, pp. 1558–1571, Jun. 2011.

Jose-Luis Lisani was born in Mallorca, Spain, in 1970. He received the Ph.D. degree in computer science and applied mathematics from Universitat de les Illes Balears, Palma, Spain, and Université Paris-Dauphine, Paris, France, in 2001.

He is currently an Assistant Professor with the Universitat de les Illes Balears. His research interests include analysis and processing of color images and video sequences.

Julien Michel received the Telecommunications Engineer degree from École Nationale Supérieure des Télécommunications de Bretagne, Brest, France, in 2006.

From 2006 to 2010, he was with Communications & Systèmes, Toulouse, France, where he worked on studies and developments in the field of remote sensing image processing. He is currently with the Centre National d'Études Spatiales, Toulouse, where he is in charge of research and development on image processing algorithms for remote sensing images.

Jean-Michel Morel was born in Maussanne, France, in 1953. He received the Ph.D. degree in applied mathematics from the University Pierre and Marie Curie, Paris, France, in 1980.

In 1979, he was an Assistant Professor with the University of Marseille Luminy, Marseille, France. In 1984, he was with Université Paris-Dauphine, Paris, where he was promoted as a Professor in 1992. Since 1997, he has been a Professor of applied mathematics with the Centre de Mathématiques et de leurs Applications, École Normale Supérieure de Cachan, Cachan, France. His research interests include mathematical analysis of image analysis and processing.

Ana Belén Petro was born in Mallorca, Spain, in 1977. She received the Ph.D. degree, in 2006, from the Universitat de les Illes Balears, Palma, Spain, where she defended her thesis in color image analysis.

She is currently an Assistant Professor with the Universitat de les Illes Balears and collaborates with the Centre de Mathématiques et de leurs Applications Laboratory, École Normale Supérieure de Cachan, Cachan, France. Her research interests include color image processing and its mathematical analysis.

Catalina Sbert was born in Mallorca, Spain, in 1964. She received the Ph.D. degree in computer science from the Universitat de les Illes Balears, Palma, Spain, in 1995.

She is currently an Assistant Professor with Universitat de les Illes Balears. Her research interests include image processing, computer vision, and the applications of partial differential equations to the aforementioned fields.